Reverse Monte Carlo simulation for the analysis of EXAFS data

1990 J. Phys.: Condens. Matter 2 9463

(http://iopscience.iop.org/0953-8984/2/48/001)

J. Phys.: Condens. Matter 2 (1990) 9463–9473. Printed in the UK

Reverse Monte Carlo simulation for the analysis of EXAFS data

S J Gurman† and R L McGreevy‡

† Department of Physics, University of Leicester, Leicester LE1 7RH, UK
‡ Clarendon Laboratory, Parks Road, Oxford OX1 3PU, UK

Received 11 June 1990

Abstract. We describe the application of the reverse Monte Carlo simulation technique to the analysis of EXAFS data. This technique generates a series of three dimensional particle configurations which are consistent with the experimental EXAFS spectrum. No input information other than the density and the chemical composition of the sample is required. We present initial results for crystalline and amorphous silicon and preliminary results for silver bromide. Since the method works directly from an experimental spectrum it promises to be extremely powerful in modelling the structures of amorphous materials.

1. Introduction

During the past ten or fifteen years the use of the technique of extended x-ray absorption fine structure (EXAFS) has become widespread in the determination of the local atomic environment in amorphous materials. The microscopic origin of EXAFS is now very well understood and detailed theories, which give good agreeement with experiment, are available in the literature and data analysis packages. These theories show that, by comparing a calculated EXAFS spectrum with experiment, detailed information may be obtained on the local atomic environment of the atom which absorbed the x-ray photon. The range of the technique is about 5 Å. The theory of EXAFS and the information that can be obtained using it have been reviewed by Hayes and Boyce (1982). The theory has recently been considered in detail by Gurman (1990) and surveys of the applications may be found in the book edited by Koningsberger and Prins (1988).

The usual aim of EXAFS studies of amorphous materials is to determine the extent and nature of the local structural order. Thus we seek information on the number, type and distance of the near-neighbours and on the variations in bond lengths and angles implicit in the lack of long range order. In determining such parameters via an analysis of the experimental data we invariably need to make some assumptions. One of the commonest in EXAFS analysis is that the peaks in the radial distribution function are Gaussian in shape. Such assumptions limit the applicability of the technique and can lead to error.

Neutron diffraction has also been extensively and very successfully used to obtain structural information on amorphous materials. Diffraction experiments give, after some small corrections, the structure factor $A(Q)$. This may be Fourier transformed,

0953-8984/90/489463+11$03.50

if the Q range of the experiment is sufficiently large, to yield the radial distribution function $g(r)$. By use of the technique of isotopic substitution we may, in favourable cases, obtain partial radial distribution functions $g_{\alpha\beta}(r)$ for multicomponent systems from which coordination numbers and interatomic distances may be derived. As is the case in EXAFS studies, extraction of the structural parameters from the experimental data involves making certain assumptions, which can lead to difficulties and possibly to error.

Recently one of us described the application of a new method of structural modelling, reverse Monte Carlo (RMC) simulation, to the analysis of neutron diffraction data (McGreevy and Pusztai 1988) and to the combination of neutron and x-ray diffraction data for amorphous materials (Keen and McGreevy 1990). The RMC method produces a three-dimensional model of the structure by fitting to either $g(r)$ or $A(Q)$. One of its advantages is that it makes very few assumptions about the structure of the samples; essentially only the density and chemical composition are required. In this paper we describe the application of this technique to the analysis of EXAFS data.

2. Conventional EXAFS analysis

EXAFS arises from the scattering of the photoelectron emitted on absorption of an x-ray photon. The scattering is off atoms surrounding the absorbing atom. To separate the scattering and absorption processes we write the photon absorption cross section $\sigma(E)$ for an atom in a solid as

$$\sigma(E) = \sigma_0(E)[1 + \chi(E)] \tag{1}$$

where E is the x-ray photon energy. $\sigma_0(E)$ is the absorption cross section for a free atom and is essentially featureless except for the threshold. (Note that both σ_0 and σ refer to the contribution of a single edge to the absorption.) $\chi(E)$, which is defined by equation (1), is the EXAFS function and represents the modulation in the photoabsorption rate due to scattering processes. The modulation arises from interference between the outgoing part of the photoelectron wavefunction and that small part of the wave which is scattered back from near-neighbour atoms. This interference process gives the oscillation in σ with increasing photon energy which is known as EXAFS.

EXAFS theories concentrate on the calculation of $\chi(E)$. This is usually written as $\chi(k)$ with k the photoelectron wavevector, since this is the parameter most directly related to the interference process. It is, of course, simply related to the photon energy. For the purposes of explanation we shall use the simplest of the theories of EXAFS, the approximate plane-wave theory, even though in practice we use the exact fast curved-wave theory. In the plane-wave approximation the EXAFS function $\chi(k)$ due to a single scattering atom at a fixed distance r from the central atom may be written as

$$\chi_1(k, r) = \frac{-A(k)}{kr^2}|f(k, \pi)|e^{-2r/\lambda}\sin(2kr + 2\delta_1 + \psi) \tag{2}$$

for K edge absorption. In this expression $f(k, \pi)$ is the electron backscattering factor for the atom at r, this being a complex number of amplitude $|f(k, \pi)|$ and phase ψ.

$f(k,\pi)$ varies both with k and the atomic number of the scattering atom. δ_1 is the phaseshift introduced by the passage of the photoelectron through the potential of the absorbing atom: for a K edge this is the $l = 1$ phaseshift (1s $\rightarrow$ p transition). λ is the elastic mean free path of the photoelectron; only elastically scattered electrons can interfere and so contribute to the EXAFS. $A(k)$ is an amplitude factor which allows for processes which contribute to photoabsorption but not to EXAFS, such as multi-electron excitations. In practice $A(k)$ is taken to be energy independent.

The measured EXAFS signal will be a sum of contributions from all scattering and central atoms. The definition of the partial radial distribution function $g_{\alpha\beta}(r)$ allows us to write this as

$$\chi_\alpha(k) = \sum_\beta \frac{-A(k)}{k} |f_\beta(k,\pi)| 4\pi\rho \int_0^\infty (g_{\alpha\beta}(r) - 1) \mathrm{e}^{-2r/\lambda} \sin(2kr + 2\delta_1 + \psi_\beta)\, \mathrm{d}r \qquad (3)$$

since we measure the EXAFS on the absorption edge of an atom of known chemical type α.

The simplest method of analysing EXAFS data is to Fourier transform it. If we transform with respect to $2kr$, equation (3) shows that the result will be a weighted sum of the $g_{\alpha\beta}(r)$ with the peaks distorted and shifted by the k dependence of $|f_\beta(k,\pi)|$ and $(2\delta_1 + \psi_\beta)$. Further distortions will be introduced by the finite data range. A better method is to transform $k\chi_\alpha(k)/|f_\beta(k,\pi)|$ with respect to $(2kR + 2\delta_1 + \psi_\beta)$ with β chosen to be the dominant atom, usually the nearest-neighbour type, and using calculated scattering data, but the results are still not very satisfactory.

Because of the unsatisfactory results given by a Fourier transform most EXAFS analyses are done by fitting $\chi(k)$ itself, using calculated electron scattering data and one of the more accurate theories (Gurman 1990). In order to do this we need to make assumptions about the shape of $g_{\alpha\beta}(r)$. By far the commonest assumption is that $g_{\alpha\beta}(r)$ may be represented as a sum of Gaussian peaks. With this assumption we may perform the integral in equation (3) to obtain what is usually considered to be the standard expression for the EXAFS function

$$\chi(k) = \sum_j \frac{-A}{k} \frac{N_j}{R_j^2} |f_j(k,\pi)| \mathrm{e}^{-2R_j/\lambda} \mathrm{e}^{-2\sigma_j^2 k^2} \sin(2kR_j + 2\delta_1 + \psi_j) \qquad (4)$$

in which j is a peak, or 'shell' index. A shell j consists of N_j atoms at a mean distance R_j from the absorbing atom and with mean square deviation σ_j^2.

Even if we use one of the exact curved-wave EXAFS theories we still use the Gaussian form for $g_{\alpha\beta}(r)$. Thus, if we write the contribution to the EXAFS of a single scattering atom at a fixed distance r as $\chi_1(k,r)$ then we can rewrite equations (3) and (4) as

$$\chi(k) = \sum_\beta 4\pi\rho \int_0^\infty r^2 (g_{\alpha\beta}(r) - 1) \chi_1(k,r)\, \mathrm{d}r \qquad (5)$$

$$= \sum_j N_j \mathrm{e}^{-2\sigma_j^2 k^2} \chi_1(k, R_j). \qquad (6)$$

Once a form for $\chi_1(k,r)$ has been decided on we fit the spectrum shell by shell using calculated scattering data. Non-Gaussian peaks may be approximately dealt with by representing them as a sum of Gaussian sub-peaks (Greaves *et al* 1988). Almost all of the standard EXAFS data analysis packages are based on equation (6); the SERC Daresbury package EXCURV88, which uses curved-wave theory for $\chi_1(k,r)$ is perhaps the best known and most widely used.

3. RMC analysis of EXAFS

The assumption of Gaussian peak shapes in the standard EXAFS analysis techniques is a possible source of error. It is clear, especially in the case of asymmetric peaks that are modelled by a set of Gaussian sub-peaks, that the resulting arrangement of coordination shells may be physically unrealistic or even impossible. In order to avoid making this assumption, and to generate coordination shells that must be physically possible, we have adapted the RMC method (McGreevy and Pusztai 1988) to the analysis of EXAFS data. This technique generates a three-dimensional model of the structure that is sufficiently large to give an accurate calculated $\chi(k)$ which can be compared with experiment.

The RMC algorithm is very simple. In summary:

1. We start with an initial configuration. This is a three-dimensional array of N points, representing atomic coordinates, in a cube of side L. The array may be generated at random, it may be a lattice, or it may be a set of coordinates generated in another simulation. The only constraint is that it must have the same chemical composition and mass density as the experimental sample.

2. Normal periodic boundary conditions are applied, i.e. the cube is surrounded by images of itself, and the radial distribution function $g_S(r)$ is calculated.

3. A new configuration is generated by random motion of one particle (point). The new radial distribution function $g'_S(r)$ is then calculated.

4. From the simulated radial distribution functions $g_S(r)$ and $g'_S(r)$ EXAFS functions $\chi_S(k)$ and $\chi'_S(k)$ are calculated using equation (5). These two functions are compared with the experimental spectrum from the system which is being modelled. We use the standard form of comparison of EXAFS spectra, with a k-weighted spectrum and normalising to the amplitude of the experimental spectrum

$$FI = \sum_i [k_i^n(\chi_S(k_i) - \chi_E(k_i))]^2/\sigma_E^2 \sum_i [k_i^n \chi_E(k_i)]^2 \tag{7}$$

where σ_E^2 is the estimated squared fractional error on the experimental spectrum. For simplicity we take this to be independent of k, as is usually the case for EXAFS spectra. The k weighting (usually with $n = 3$) is used to give each point in the spectrum approximately equal amplitude. We calculate FI and FI', the fit indices for the two calculated spectra $\chi(k)$ and $\chi'(k)$.

5. If $FI < FI'$ then the new configuration is accepted. If $FI > FI'$ then the new configuration is accepted with probability $\exp[-(FI - FI')]$.

6. If the new configuration is accepted then it becomes the starting configuration, otherwise the old configuration is retained. We then repeat from step 3.

7. The process is repeated until FI converges, i.e. until we reach equilibrium. If the simulated spectrum is in agreement with the experiment then FI will have a value of order unity. If this is the case at convergence we continue, saving approximately one accepted configuration in N. These are deemed to be statistically independent. The $\chi(k)$ calculated from *each* of these accepted configurations agrees with experiment to within a known error. *Each* configuration is a valid model of the system and can be used to determine structural parameters.

4. Calculation details

When we begin the simulation process it is necessary to calculate $g_S(r)$ in the normal way, using the $\frac{1}{2}N(N-1)$ interparticle distances. However, between each step, it is only necessary to calculate the *change* in $g_S(r)$ due to the movement of a single particle. This involves N interparticle distances. By doing this we save a considerable amount of computer time and so can make N large; we use 1000 atoms in the basic cube of side L. This also means that we can calculate $g_S(r)$ out to a fairly large distance without running into problems with the periodic boundary conditions.

$g_E(r)$ is zero below a certain minimum value of r, r_0, since particles in the real system can only approach to within a closest distance determined by the atomic radii. We can therefore automatically reject a new configuration at step 3, before calculating $g'_S(r)$, if the moved particle goes within r_0 of any other particle. In compounds we define an r_0 for each partial radial distribution function; it is usually set at 80–90% of the distance of the first peak in the partial radial distribution function.

In a conventional Monte Carlo simulation the maximum distance that a particle is moved between two configurations is chosen in order to make the ratio of accepted and rejected configurations take a value such as 0.5. In the RMC simulation this has been found to be inefficient, since it results in a small maximum movement. Instead the maximum has been chosen to be 'physically reasonable', 0.5 Å. The acceptance ratio is then about 0.1 but the calculation is sufficiently rapid for an adequate number of acceptable configurations to be generated. Also, with this large value for the maximum distance moved, major rearrangements of the set of N points are possible, so escape from local minima in FI can occur.

The estimated squared fractional error on the experimental spectrum, σ_E^2, is taken to be independent of k and may be obtained from the counting statistics of the EXAFS experiment. A value of 10^{-4} (noise level of 1%) is appropriate for our data.

In using equation (5) to calculate $\chi_S(k)$ we need a good calculation of the EXAFS due to a single scattering atom. We have used spectra calculated using the single-scattering fast curved-wave theory (Gurman *et al* 1984) by the Daresbury data analysis package EXCURV88. This automatically calculates a spectrum at the same k values as appear in the experimental spectrum. We have calculated $\chi_1(k,r)$ at a range of r values separated by 0.1 Å, corresponding to the distance values in the $g(r)$ histogram. These were then input into the program and used in the form of a look-up table so that $\chi_S(k)$ could be calculated rapidly from the $g_S(r)$ histogram.

(For a more detailed description of the principles and practice of the RMC method see McGreevy *et al* (1990).)

5. Results for amorphous and crystalline silicon

In order to test the RMC simulation technique on real EXAFS data we have analysed spectra from crystalline and amorphous silicon. The amorphous silicon sample was in the form of a sputtered thin film. Spectra were obtained on the SRS at SERC Daresbury as part of a study of amorphous silicon alloys. Details of the sample preparation and experiment may be found elsewhere (Bayliss and Gurman 1990). The spectra were fitted using the standard EXCURV88 program with the results given in table 1. For the analysis of amorphous silicon data our starting configuration was that of a perfect

Table 1. Details of EXCURV88 and RMC fits. (*a*) Fits using EXCURV88; (*b*) Fits using RMC

	c-Si			a-Si		
Shell	R (Å±0.02)	N	σ^2 (10^{-4} Å^2)	R (Å±0.02)	N	σ^2 (10^{-4} Å^2)
(*a*)						
1	2.33	4 ± 1	50 ± 15	2.35	4 ± 1	65 ± 15
2	3.82 ± 0.02	9 ± 5	85 ± 80			
3	4.48 ± 0.02	≈ 12	≈ 100			
$V_i = -4$ eV	AFAC = 0.65					
(*b*)						
1	2.35	4	25	2.35	4	25
2	3.9	12	100	≈ 4.1		≈ 1000
3	4.5	12		≈ 4.1		≈ 1000
Bond angle:	c-Si $109 \pm 3°$		a-Si $109 \pm 15°$			

silicon crystal. The final configuration obtained for amorphous silicon was used as the starting point for the simulation of crystalline silicon.

In the RMC simulation we used $N = 1000$ atoms, corresponding to a cell length $L = 27.5$ Å. The EXAFS was fitted out to a distance of 6 Å, beyond any discernible feature in the Fourier transform of the experiment, and r_0 was set at 2 Å. In figure 1(*a*) we show the simulated $g_S(r)$ for crystalline and amorphous silicon obtained by averaging over five converged configurations. Figure 1(*b*) shows the distance integrated $g_S(r)$; the fourfold coordination is apparent. Figure 2(*a*) compares the experimental EXAFS spectrum for amorphous silicon with that obtained from RMC whilst figure 2(*b*) shows the result of a fit using EXCURV88. The quality of the two fits is very similar. We deliberately chose a spectrum containing an experimental 'glitch' (at about 13 Å^{-1}) in order to test the technique. Clearly this artefact causes no problems.

The program was run on the CONVEX C220 at SERC Daresbury using an optimizing compiler. About 15000 total configurations, and some 1500 accepted configurations, could be obtained in 3 minutes of CPU time. Convergence took about 10 minutes CPU time for both samples and another 15 minutes was used to obtain several (usually 5) $g_S(r)$ for averaging. These timings suggest that the technique should be widely applicable.

The radial distribution functions shown in figure 1(*a*) demonstrate that the nearest neighbour shells in crystalline and amorphous silicon are almost identical, a conclusion also reached by standard EXAFS analyses (see table 1). The comparatively large step length prevents us from determining the mean square deviation in bond length, σ_1^2, with any precision but RMC gives much the same value as that obtained using EXCURV88, $\sigma_1^2 = 0.005$Å^2 corresponding to $\sigma_1 = 0.07$ Å. The second- and third-neighbour peaks clearly appear in the $g(r)$ for crystalline silicon, at the correct distances, but are merged in the $g(r)$ for amorphous silicon. The widths of the $g(r)$ peaks in crystalline silicon agree with those found using EXCURV88. The position and width of the second-neighbour peak allow us to calculate the value of the bond angle in crystalline silicon and its range due to thermal motion. We find a bond angle of 109° with a range of ±3°.

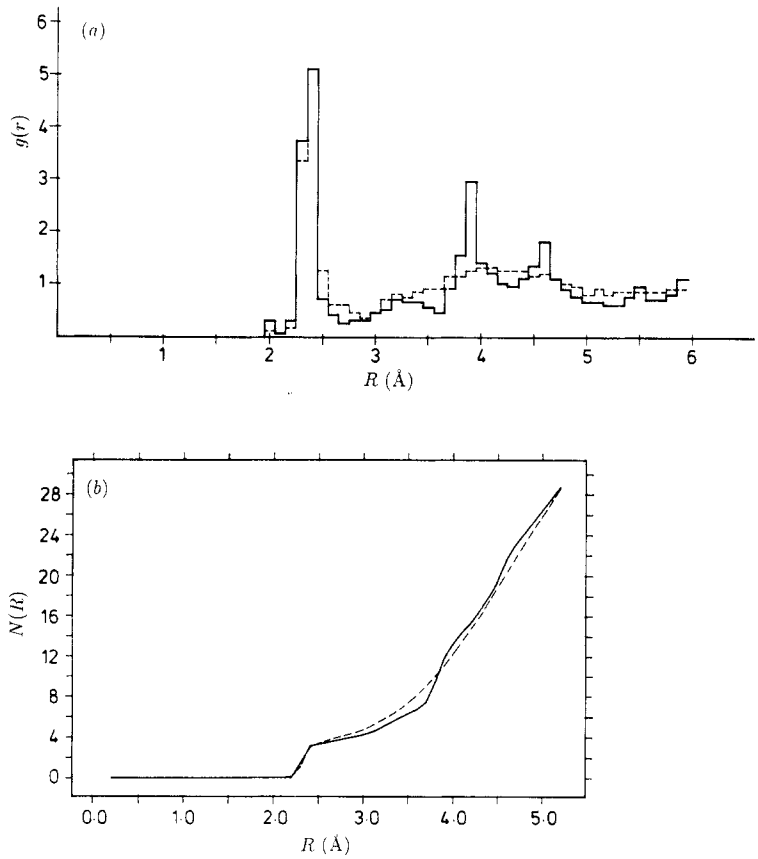

Figure 1. (*a*) Radial distribution functions for crystalline (full line) and amorphous (broken line) silicon obtained from RMC analyses of the EXAFS data. (*b*) The integrated $g(r)$ showing fourfold coordination of Si.

Figure 3 shows the bond angle distribution calculated directly from the 1000 atoms in the RMC simulation. We define a bonded atom as one lying between 2.2 and 2.5 Å from a given atom. We then find that 95% of the atoms are fourfold coordinated in both crystalline and amorphous silicon. The thermal range of the bond angle in crystalline silicon is apparent in figure 3. It is also apparent that the range of bond angles in amorphous silicon is very much wider, although the mean bond angle is unaltered at the tetrahedral value of 109°. The RMC range of bond angles in our sputtered amorphous silicon sample is 15°, rather larger than is usually found but sputtered samples are known to be highly disordered. The bond angle in amorphous silicon could not be determined using EXCURV88 because the second-neighbour shell was too weak to fit it.

The RMC simulation technique clearly provides a good fit to EXAFS data from crystalline and amorphous silicon and gives good structural information. The simulation provides us with a picture of the amorphous material whose structure is seen to be a continuous random network with a rigid bond length but much bond angle distortion which destroys long-range order.

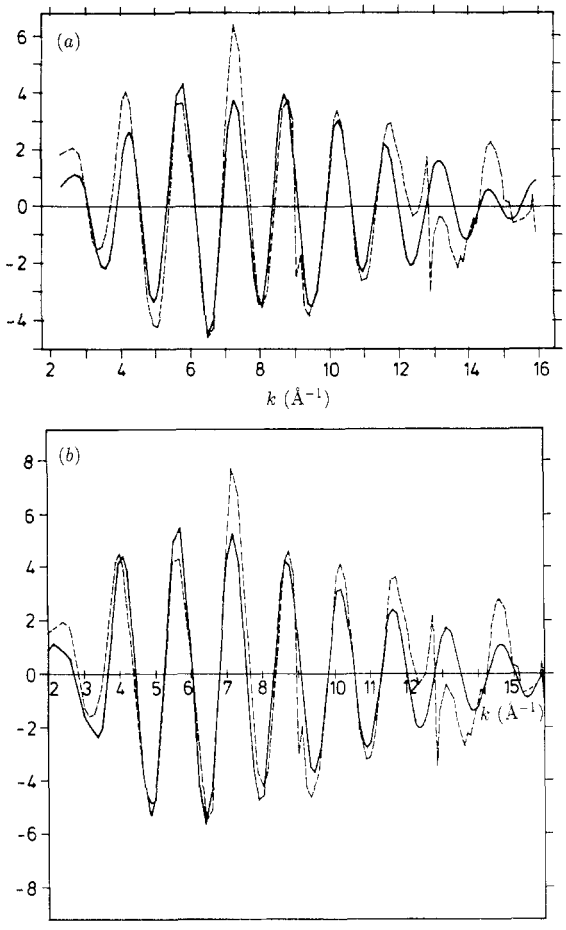

Figure 2. (*a*) Experimental (broken curve) and RMC fitted (full curve) EXAFS spectra (weighted by k^3) for amorphous silicon. (*b*) As (*a*), but fitted using the standard EXCURV88 package.

6. Results for silver bromide

We have also used the RMC technique to attempt an analysis of the EXAFS on the Br K edge of silver bromide. The EXAFS data, taken at 18 and 100 K at SERC Daresbury, were kindly provided by Dr D Batchelor of the University of Cambridge. The analysis of these spectra is continuing, but our preliminary results show some interesting features of the RMC simulation.

The Br K edge EXAFS contains information on Br–Ag and Br–Br correlations only; Ag–Ag correlations are completely undefined. Thus a single EXAFS spectrum contains less information than a neutron diffraction experiment. In performing the RMC simulation we first tried setting the cut-off distance at somewhat less than the Br–Ag nearest-neighbour distance of 2.89 Å, $r_0 = 2.3$ Å for all three partial radial distribution functions. Although the simulation converged reasonably well, and gave a strong peak in $g_{\mathrm{BrAg}}(r)$ at the correct distance, there was considerable cross talk between the partial radial distribution functions, both $g_{\mathrm{BrBr}}(r)$ and $g_{\mathrm{AgAg}}(r)$ being about unity in the region of the nearest-neighbour peak (see figure 4). These two

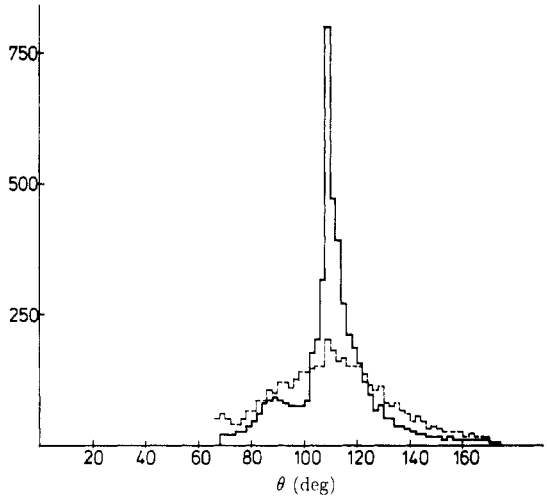

Figure 3. Bond angle distributions in crystalline (full line) and amorphous (broken line) silicon obtained from the RMC simulation.

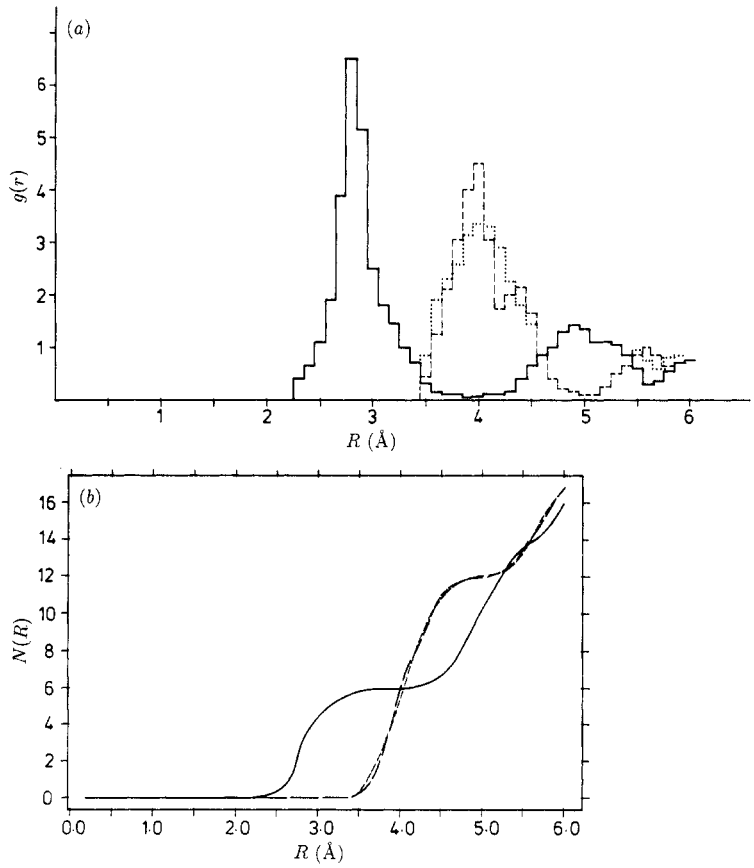

Figure 4. (*a*) Partial radial distribution functions $g_{\alpha\beta}(r)$ for crystalline AgBr at 100 K obtained from RMC simulation of EXAFS data from the bromine K edge. Full line: Br–Ag; broken line: Br–Br; dotted line: Ag–Ag. (*b*) Integrated $g_{\alpha\beta}(r)$.

distributions were flat and so $g_{BrBr}(r)$ did not contribute significantly to the EXAFS.

Clearly one EXAFS spectrum does not constrain the three partial radial distribution functions of a binary material sufficiently. However if we set $r_0 = 2.3$ Å for $g_{BrAg}(r)$ and 3.5 Å for the other two partials then we found that the cross talk was totally eliminated. The result of a fit to the 100 K data is shown in figure 5. The prevention of close like-atom correlation and the overall density constraint suffice to define the system enough to enable the single EXAFS data set to correctly separate the three partials. A similar result is found in RMC simulation of neutron diffraction data for molten salts (McGreevy and Pusztai 1990).

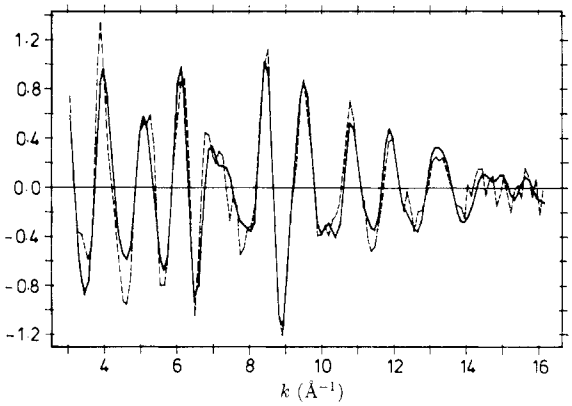

Figure 5. Experimental (full curve) and RMC fitted (broken curve) EXAFS spectrum (weighted by k^2) from the Br K edge in AgBr at 100 K.

In order to improve the analysis of the structure of materials containing more than one type of atom we should fit EXAFS data from the absorption edges of several types of atom simultaneously. We are at present engaged in developing the program to do this for binary materials.

7. Conclusions

We have described the application of the reverse Monte Carlo simulation technique to the analysis of EXAFS data. The algorithm is simple and we have shown that it is sufficiently fast to be widely applicable. The chief advantage of the technique lies in its lack of assumptions about the shape of the radial distirbution functions. We therefore expect it to be most widely used in those situations where the assumptions of standard EXAFS theory, particularly the Gaussian shape of the peaks in the radial distribution function, are but poorly obeyed. Two clear examples are the structures of metallic glasses and molten materials (McGreevy and Pusztai 1990). The sequential nature of the fitting process in RMC suggests that it will also be useful in analysing data taken sequentially. Examples of this might be the so-called quick EXAFS method (Frahm 1989) or in following a material through the melting point (Orton 1990). We are still developing the program and intend to report applications of RMC to these systems in due course. Another advantage of the technique is the ability to combine EXAFS and other experimental data, e.g. neutron and x-ray diffraction. This should

prove useful for investigating amorphous materials, particularly those with complex chemical compositions.

References

Bayliss S C and Gurman S J 1990 *J. Non-Cryst. Solids* at press

Frahm R 1989 *Rev. Sci. Instrum.* **60** 2515

Greaves G N, Gurman S J, Gladden L F, Spence C A, Cox P, Sales B C, Boatner L A and Jenkins R N 1988 *Phil. Mag.* B **58** 271

Gurman S J 1990 *Synchrotron Radiation and Biophysics* ed S S Hasnain (Chichester: Ellis-Horwood) ch 1

Gurman S J, Binsted N and Ross I 1984 *J. Phys. C: Solid State Phys.* **17** 143

Hayes T M and Boyce J B 1982 *Solid State Physics* vol 37 (New York: Academic) p173

Keen D A and McGreevy R L 1990 *Nature* **344** 423

Koningsberger D C and Prins R (ed) 1988 *X-ray Absorption* (Chichester: Wiley)

McGreevy R L, Howe M A, Keen D A and Clausen K N 1990 *Neutron Scattering Data Analysis (IOP Conference Series)* ed M W Johnson (Bristol: IOP Publishing) in press

McGreevy R L and Pusztai L 1988 *Mol. Simul.* **1** 359

—— 1990 *Proc. R. Soc.* A in press

Orton B R 1990 *Neutron and X-ray Scattering (IOP Conference Series 101)* ed M C Fairbanks, A N North and R J Newport (Bristol: IOP Publishing) p 77